Virology 483 (2015) 1–12

Contents lists available at ScienceDirect

Virology

journal homepage: www.elsevier.com/locate/yviro

Global profiling of histone modifications in the polyomavirus BK virion minichromosome

Chiung-Yao Fang [a], Cheng-Huang Shen [b], Meilin Wang [c], Pei-Lain Chen [d], Michael W.Y. Chan [e], Pang-Hung Hsu [f,*], Deching Chang [e,**]

[a] Department of Medical Research, Chia-Yi Christian Hospital, Chia-Yi, Taiwan
[b] Department of Urology, Chia-Yi Christian Hospital, Chia-Yi, Taiwan
[c] Department of Microbiology and Immunology, Chung Shan Medical University, Taichung, Taiwan
[d] Department of Medical Laboratory Science and Biotechnology, Central Taiwan University of Science and Technology, Taichung, Taiwan
[e] Institute of Molecular Biology, National Chung Cheng University, 168 University Rd., Min-Hsiung, Chia-Yi 621, Taiwan
[f] Department of Bioscience and Biotechnology, National Taiwan Ocean University, 2 Pei-Ning Rd., Keelung 202, Taiwan

ARTICLE INFO

Article history:
Received 29 November 2014
Returned to author for revisions
5 January 2015
Accepted 8 April 2015
Available online 15 May 2015

Keywords:
Histone modification
Nucleosome
Proteomics
BKPyV
Minichromosome
LC–MS/MS

ABSTRACT

During polyomavirus infection, the viral DNA adopts histones from host cells and forms minichromosomes as an important part of the viral life cycle. However, the detailed mechanisms of this histone incorporation remain unclear. Here, we profiled the histone posttranslational modifications (PTMs) in BKPyV minichromosomes and in the chromatin of BKPyV host cells. Through Triton-acetic acid-urea (TAU)-PAGE separation followed by nanoflow liquid chromatography coupled with tandem mass spectrometry (LC–MS/MS) analysis, we identified different kinds of PTMs on histones from BKPyV minichromosomes and from host cells. We observed not only the common PTMs on histones such as acetylation, methylation, phosphorylation, ubiquitination, and formylation but also several novel PTM sites. Our results also confirmed that the BKPyV minichromosome is hyperacetylated. Our detailed histone PTM profiles for the BKPyV minichromosome provide insights for future exploration of the underlying mechanisms and biological relevance of these histone PTMs.

Introduction

The basic structure of chromatin is the nucleosome, assembled from 146 bp of DNA and an octamer complex of core histone proteins containing two copies of H2A, H2B, H3, and H4 (Kornberg, 1974; Kornberg and Lorch, 1999; Luger et al., 1997). The N-terminus of the histones extends outside the histone octamer and is the major region where posttranslational modifications (PTMs) take place (Cheung et al., 2000a). To date, more than eight types of histone PTMs have been reported, including acetylation, methylation, phosphorylation, ubiquitination, sumoylation, ADP-ribosylation, deimination, and proline isomerization (Kouzarides, 2007). Histone PTMs at certain loci affect the higher-order structures of chromatin and serve as signals for protein recognition. In addition, histone PTMs play major roles in several important cellular processes, such as recruitment of effector proteins to DNA regions, chromatin compaction, and regulation of gene transcription, as well as regulation of the cell cycle and cell growth, differentiation, and apoptosis (Jenuwein and Allis, 2001; Strahl and Allis, 2000; Wang and Patel, 2011). Therefore, the identification of PTMs on histones is a pivotal aspect in the study of gene regulation.

During infection by viruses, the host cells' machinery is utilized for viral propagation and completion of the viral life cycle. Besides depending on functions that are controlled by the host chromatin, viruses have also developed unique mechanisms to regulate chromatin structure and function as a way to control their life cycles. Previous studies have reported the assembly of viral nucleosomes in several different viruses, such as polyomaviruses (Prieto-Soto et al., 1983), simian virus 40 (SV40) (Griffith, 1975), human and bovine papillomaviruses (HPV and BPV) (Favre et al., 1977; Rosl et al., 1986), adenovirus (Tate and Philipson, 1979), latent Epstein-Barr virus (EBV) (Shaw et al., 1979), herpes simplex virus (HSV)-1 (Deshmane and Fraser, 1989), and hepatitis B virus (HBV) (Bock et al., 1994). Importantly, the histone PTMs on viral nucleosomes are highly correlated with the stage of the viral life cycle. For example, the genome of HSV-1 forms an ordered nucleosome structure when the virus infects a sensory neuron and exists in a latent state (Deshmane and Fraser, 1989) but not when it enters the lytic stage (Leinbach and Summers, 1980; Muggeridge and Fraser, 1986), and the HSV-1 genome has been

* Corresponding author. Tel.: +886 2 2462 2192x5567; fax: +886 2 2462 2320.
** Corresponding author. Tel.: +886 5 2720411x66500; fax: +886 5 2722871.
E-mail addresses: phsu@ntou.edu.tw (P.-H. Hsu), biodcc@ccu.edu.tw (D. Chang).

http://dx.doi.org/10.1016/j.virol.2015.04.009
0042-6822/

shown to exhibit differential levels of the histone activation marks, histone H3 Lys9 and Lys14 acetylations, during the latent and lytic stages of infection (Kent et al., 2004). Similarly, highly acetylated histones H3 and H4 in the minichromosome has been found to represent the active transcription or replication state of HBV (Belloni et al., 2009; Pollicino et al., 2006), and the viral life cycle of HPV has also been correlated with dynamic changes in histone PTMs (Wooldridge and Laimins, 2008). The polyomaviral minichromosome is assembled when host histones are encapsulated into the virion and are wrapped up by the viral genome (Tan, 1977; Waga and Stillman, 1998). Polyomaviruses regulate host cell chromatin and alter viral minichromosome status in the course of completing their life cycle, suggesting similar mechanisms of chromatin regulation for both the viral minichromosomes and their host cells. Although some histone PTMs of polyomavirus have been investigated (Balakrishnan et al., 2010; Balakrishnan and Milavetz, 2005; Milavetz, 2004; Milavetz et al., 2012), the global profiling of histone modifications in polyomavirus remains absent.

The human polyomavirus BK (BKPyV) is found in the kidney and causes polyomavirus-associated nephropathy in renal transplantation patients (Ramos et al., 2002; Ramos and Hirsch, 2006). The presence of virally encoded miRNA in the latent stage of BKPyV infection indicates that the BKPyV life cycle is regulated at the epigenetic level (Broekema and Imperiale, 2013). Mass spectrometry, a detection method of high accuracy and sensitivity, has been intensively used in recent years in the identification of protein PTMs (Britton et al., 2011; Garcia et al., 2006; Gilmore and Washburn, 2007). Our recent evidence that the BKPyV genomic DNA is not being methylated during infection (Chang et al., 2011) raises the possibility that histone PTMs may play pivotal roles in the BKPyV life cycle. In the current study, we profiled the histone PTMs on BKPyV minichromosomes by performing Triton-acetic acid-urea (TAU)-PAGE separation followed by mass spectrometry. The results we obtained can serve as the foundation for future mechanistic studies.

Results

TAU-PAGE analysis of histones in BKPyV virions and host cells

The purification profile of BKPyV virions is shown in Supplementary Fig. 1, including the $OD_{260/280}$ ratio, particle density and hemagglutination assay (HA) (Supplementary Fig. 1A). The purity of BKPyV virions is demonstrated by SDS-PAGE and Coomassie blue staining (Supplementary Fig. 1B). According to our previous results of Western blot (Fang et al., 2010), the additional bands are fragments of capsid proteins. In order to profile the histone PTMs present in BKPyV minichromosomes and in BKPyV's host cells, we employed TAU-PAGE to separate the modified histone species, followed by mass spectrometry analysis to identify the sites and types of the PTMs. Acid-extracted histone samples from BKPyV virions and uninfected host Vero cells were subjected to TAU-PAGE separation. As visualized by Coomassie blue staining, the overall pattern of histone bands was different between BKPyV minichromosomes and host chromatin (Fig. 1A). The banding profiles of individual histone subunits were identified by western blotting with specific antibodies against histones H2A (Fig. 1B), H2B (C), H3 (D), and H4 (E). We found that histone subunits extracted from BKPyV virions showed higher band positions on TAU gels than those extracted from host cells. We also found that H3 and H4 in BKPyV were higher amount than in Vero. To examine the differences in histone patterns between BKPyV virions and host cells, the major bands observed in TAU-PAGE were subjected to in-gel digestion and LC–MS/MS analysis to identify the PTMs they contained.

Identification of PTMs on histone H2A

Histone H2A, a subunit of the core histone octamer, consists of a main globular domain with extended tails on both N- and C-termini. Both histone tails can extend outside of the nucleosomal space and help maintain nucleosome structure (Luger et al., 1997). In this study, one additional band for histone H2A in BKPyV virion extract was identified as compared with Vero cell extract (Fig. 1B). N-terminal acetylation of histone H2A was further demonstrated only in BKPyV virions (Table 1). Most of the PTMs identified on histone H2A were located in the N- and C-terminal tails (Fig. 2). Acetylation marks were identified on three H2A lysine residues, Lys5, Lys9, and Lys36. We further determined that these three acetylations occurred sequentially: Lys36 was the first to be acetylated, followed by Lys5 and Lys9. The acetylation for N-terminal and Lys5 in histone H2A was demonstrated in Supplementary Fig. 2. The double acetylation of Lys5 and Lys9 was found in the hyperacetylated form of H2A in both Vero and BKPyV virions (Supplementary Fig. 3). In addition, we identified one formylation mark on Lys36, but found no correlation between acetylation and formylation at Lys36. Several PTMs were identified on Lys118 of H2A, including mono-methylation, di-methylation, and ubiquitination. A previous study has correlated H2A ubiquitination at Lys119 with gene inactivation (Zhou et al., 2008). The ubiquitination of Lys118 was found in both host and BKPyV H2A (Supplementary Fig. 4); however, the ubiquitination on Lys119 was only found in host H2A but not on BKPyV H2A (Supplementary Fig. 5).

Identification of PTMs on histone H2B

The histone H2B bands observed in TAU-PAGE (labeled 0 through 7 in Fig. 1C) were trypsin-digested and analyzed by LC–MS/MS. We identified the following PTMs on the histone H2B of BKPyV virions (with those PTMs not found on host cell H2B indicated in italics): acetylations at the *N-terminus* and on Lys5, Lys11, Lys12, Lys15, Lys16, Lys20, Lys23, *Lys34*, *Lys46*, *Lys116*, and Lys120; methylations on Lys5 and Arg72; a di-methylation on Lys108; a phosphorylation on *Ser6*; a formylation on *Lys34*; and ubiquitinations on *Lys108* and Lys120 (Table 2). Several PTMs on H2B of BKPyV virions were characterized, such as acetylations at the N-terminus (Supplementary Fig. 6), acetylation on Lys34 (Supplementary Fig. 7), Lys46 (Supplementary Fig. 8), Lys116 (Supplementary Fig. 9). A novel serine phosphorylation site, Ser6, was identified on BKPyV H2B (Supplementary Fig. 10).

Hyperacetylated H2B was previously found in SV40 and has been suggested to help maintain the SV40 minichromosome in an active state (Chestier and Yaniv, 1979). Our current mass spectrometry analysis identified more than 9 acetylation marks on lysine residues in BKPyV H2B. These acetylation marks were mainly located in the N-terminal tail and the core domain of H2B (Table 2 and Fig. 3). After examining the results for the different H2B subspecies, we concluded that the acetylations on H2B took place sequentially. Lys20 was the first to be acetylated, followed by the N-terminus and Lys16. The next acetylations occurred at Lys5, Lys34, and Lys120. In the final stage, Lys12, Lys23, Lys46, and Lys116 were acetylated (Fig. 3, bands H2B-0 through H2B-3). In addition, H2B extracted from BKPyV virions had a higher level of acetylation than that extracted from host cells. For example, 9 lysine residues were found to be acetylated in BKPyV H2B band 3, but only 6 acetylated lysines were characterized in host H2B band 4. The biological significance of H2B hyperacetylation in BKPyV needs to be further studied.

Other PTMs were also detected on histone H2B besides acetylation. One of them was a new serine phosphorylation site, Ser6, on BKPyV H2B (band 3 seen in TAU-PAGE). Although the biological function of this serine phosphorylation is still unclear, our data showed that it may be correlated with Arg72 methylation on

BKPyV H2B, and indicated that Ser6 phosphorylation, Lys108 ubiquitination, and Lys108 mono- and di-methylation occurred only after Arg72 methylation had taken place (Fig. 3, band H2B-3). The correlation between phosphorylation, methylation, and ubiquitination at Ser6, Arg72, and Lys108 needs further investigation. We also found the H2B methylation pattern to be different between BKPyV virions and host cells. After examining the results for the different H2B subspecies, we concluded that the methylation marks on H2B were added sequentially, with Lys5 being the first to be methylated, followed by Arg72 and Lys108 (Fig. 3, bands H2B-0 and H2B-3). However, the methylation on the core-domain residue Arg72 preceded that on the N-terminal-tail residue Lys5 in host cell H2B. Yet another lysine PTM we found on H2B was ubiquitination. Other than the well-known Lys120 residue, a new ubiquitination site, Lys108, was identified in both BKPyV and host H2B subspecies (Fig. 3, band H2B-2). The biological relevance of the different methylation sequences as well as of Lys108 ubiquitination on H2B in BKPyV requires further study.

Identification of PTMs on histone H3

Using chromatin immunoprecipitation analysis, a previous study showed that the minichromosome of the nontransforming *hr-t* mutant of polyomavirus had higher levels of histone H3 methylation at Lys9 and Lys79 than that of the wild-type virus. This result suggested that epigenetic changes in H3 may affect viral physiology (Dahl et al., 2007). Another study found that histone H3 extracted from polyomavirus and SV40 had higher acetylation levels than H3 from host cells (Chestier and Yaniv, 1979). In the current study, the hypermethylation and hyperacetylation status of histone H3 from BKPyV virions was further ascertained by LC – MS/MS. We analyzed the major histone H3 band and all H3 subspecies observed in TAU-PAGE (labeled 0 through 7 in Fig. 1D). The PTMs we identified on the histone H3 of BKPyV virions (with those PTMs not found on host cell H3 shown in italics) included acetylations on *Lys9*, Lys14, *Lys18*, Lys23, Lys27, Lys36, and Lys56; methylations on *Lys5*, *Lys9*, *Lys18*, Lys27, Lys36, Arg42, and Lys79; di-methylations on *Lys9*, Lys27, Lys36, and Lys79; tri-methylations on *Lys9*, Lys27, and Lys36; and phosphorylations on *Ser10* and *Thr22*. These PTMs are summarized in Table 3, and their relative positions in histone H3 are illustrated in Fig. 4. Six lysine acetylation sites were identified in BKPyV histone H3 N-tail, such as Lys 9, Lys14 (Supplementary Fig. 11), Lys18 (Supplementary Fig. 12), Lys23 (Supplementary Fig. 13), Lys27 (Supplementary Fig. 14), and Lys36. The acetylation of lysine in BKPyV histone H3 N-tail was happened sequentially (from band H3-0 through band H3-4) with the initial acetylation occurring on Lys27 and Lys23, followed by Lys18 and Lys14 and then Lys9 and Lys36. Therefore, no single acetylation on Lys9 and Lys36 was found. Histone peptides with double acetylation on lysine were illustrated here, acetylation on both Lys9 and Lys14 (Supplementary Fig. 15) and on both Lys18 and Lys23 (Supplementary Fig. 16). The methylation on Lys79 was found in all BKPyV histone H3 subspecies (Supplementary Fig. 17).

Our results identified several lysine acetylations in the N-terminal tail of histone H3 extracted from BKPyV virions but only two lysine acetylation, Lys14 and Lys27, on host cell histone H3. Like the acetylated lysines in BKPyV histone H2B, the lysine residues in BKPyV histone H3 were acetylated sequentially (band H3-0 through band H3-4), with the initial acetylation occurring on Lys27 and Lys23, followed by Lys18 and Lys14 and then Lys9 and Lys36. Interestingly, this phenomenon was only observed in histone H3 extracted from BKPyV virions and not in host cell H3. The biological significance of this sequential acetylation needs to be further examined.

Besides lysine acetylation, lysine methylation was another important PTM found on histone H3 from both BKPyV virions and host cells. Some lysine residues in the N-terminal tail region, such as Lys5, Lys9, and Lys18, were methylated only in BKPyV H3 and not in host H3 (Fig. 4). Interestingly, all BKPyV histone H3 subspecies contained the Lys79 methylation. This methylation is known to be involved in many important biological functions, such as transcriptional regulation, cell cycle regulation, and DNA damage response (Nguyen and Zhang, 2011). In addition, we identified a novel arginine methylation site with unknown biological function, Arg42, which was methylated in host cell histone H3 subspecies but not in BKPyV H3 (Fig. 4, bands H3-0, H3-1, and H3-3). As for the phosphorylation of histone H3, we found that Ser10 was phosphorylated in BKPyV H3 but not in host H3. According to a previous study, Ser10 phosphorylation of histone H3 can be initiated by the polyomavirus small t antigen (Dahl et al., 2007). Moreover, we found a novel site of histone H3 phosphorylation, Thr22. The biological functions of the new histone H3 methylation and phosphorylation sites we identified need to be addressed by further study.

Identification of PTMs in histone H4

A previous study has suggested that the histone H4 in the minichromosomes of SV40 and wild-type polyomavirus are hyperacetylated (Schaffhausen and Benjamin, 1976). During the lytic phase, hyperacetylated histone H4 is redistributed in the minichromosome (Balakrishnan and Milavetz, 2005). Additionally, the different methylation patterns observed in SV40 histone H4 during early and late stages of infection indicated that the progression of the SV40 life cycle is dependent on histone remodeling (Balakrishnan et al., 2010). In order to profile the PTMs on BKPyV histone H4, we analyzed all H4 subspecies observed in TAU-PAGE (labeled 0 through 4 in Fig. 1E) by LC – MS/MS. As summarized in Table 4 and Fig. 5, the PTMs we identified on BKPyV histone H4 (all of which were also found on host H4) included acetylations at the N-terminus and on Lys5, Lys8, Lys12, Lys16, Lys31, and Lys59; methylations on Arg3, Lys20, Arg23, Arg55, and Lys77; di-methylations on Lys20 and Arg23; and formylations on Lys31, Lys59, Lys77, Lys79, and Lys91. Several lysines on Histone H4 N-tail were characterized to be acetylated, such as Lys5, Lys8 (Supplementary Fig. 18), Lys12 (Supplementary Fig. 19), and Lys16. We determined that the histone H4 was acetylated sequentially, first at Lys12 and then at Lys16, Lys8, and Lys5. Therefore, there is no single acetylation of Lys 5 can be found. The double acetylation on Lys12 and Lys16 (Supplementary Fig. 20), on Lys8 and Lys12 (Supplementary Fig. 21), and on Lys5 and Lys8 (Supplementary Fig. 22) were illustrated. The triple acetylation on Lys8, Lys12, and Lys16 was also demonstrated (Supplementary Fig. 23). The acetylation on Lys31 (Supplementary Fig. 24) was found in Histone H4 subspecies with lower acetylation level (H4-0 and H4-1) but not in the subspecies with higher acetylation level.

All of the acetylation sites we observed on histone H4 have been reported previously except for one new acetylation site, Lys31. After a careful examination of the sites, we determined that histone H4 was acetylated sequentially, first at Lys12 and then at Lys16, Lys8, and Lys5. This acetylation sequence accords with that determined in a human cell line (Zhang et al., 2007), providing evidence that the acetylation machinery for BKPyV histone H4 modification was completely adapted from the host cells because the original host PTM pattern was preserved. For those peptides including Lys-8 and Lys-12, the acetylation of Lys-12 but not Lys-8 was observed in the lower acetylated band of TAU gel. In the next band of TAU gel, peptides with the same amino sequence were found to contain acetylation on both Lys-12 and Lys-8, then, we can conclude that the acetylation sequence should be Lys-12 first followed by Lys-8. Another interesting finding was that the acetylation on Lys31 had to be removed (i.e., deacetylated) before

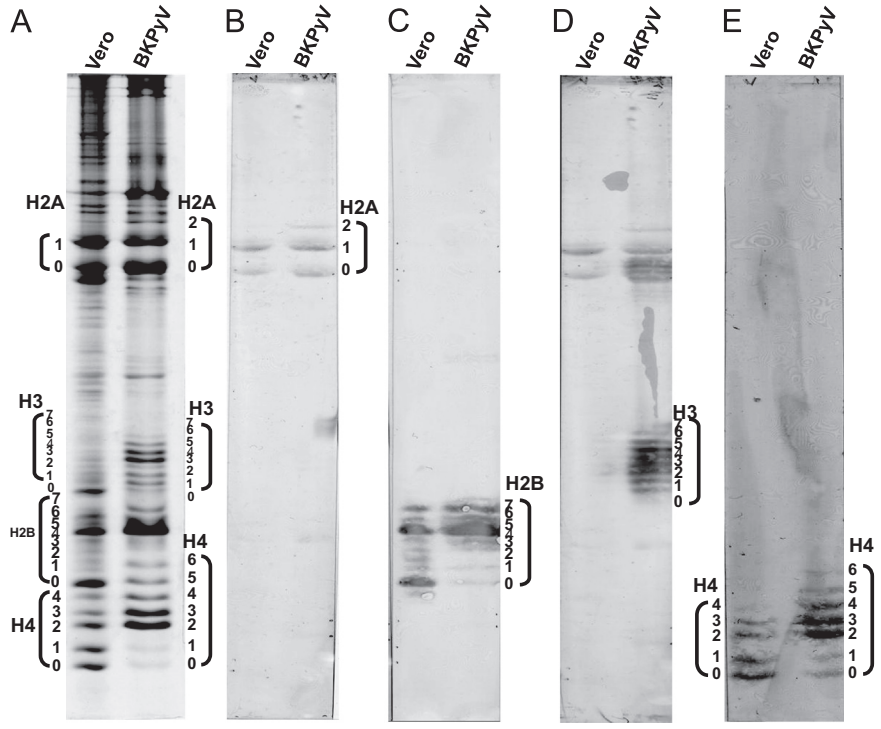

Fig. 1. Triton-acetic acid-urea (TAU)-PAGE analysis of histone acid extracts from BKPyV minichromosomes and host Vero cells. The gel images shown correspond to Coomassie blue staining (A) and immunoblotting with antibody against histone H2A (B), H2B (C), H3 (D), or H4 (E).

Table 1
Posttranslational modifications identified on histone H2A of BKPyV minichromosome and host Vero cells.

Subspecies	H2A-0[a]		H2A-1		H2A-2	
Modification site	Vero	BKV	Vero	BKV	Vero	BKV
H2A N-						Ac
K5			Ac			Ac
K9			Ac			Ac
K36	Ac[d], Formyl	Ac, Formyl[e]	Formyl	Ac, Formyl		Ac, Formyl
K118			Ubiq, Me[b]	Me2[b]		Ubiq
K119			Ubiq[c]			
H2A.Z K4			Ac	Ac		Ac
K7			Ac	Ac		Ac
K11			Ac	Ac		Ac

[a] Histone H4 subspecies (as labeled in Fig. 1B).
[b] Me: methylation; Me2: di-methylation.
[c] Ubiq: ubiquitination.
[d] Ac: acetylation.
[e] Formyl: formylation.

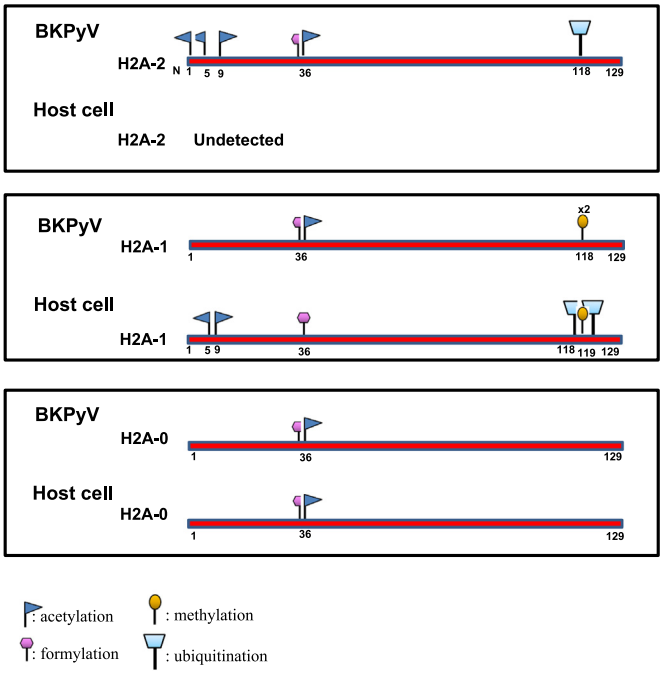

Fig. 2. Schematic illustration of histone modifications identified in histone H2A from BKPyV minichromosome and acid-extracted Vero cell histones.

acetylation at Lys5 and Lys8 could take place. The role of Lys31 acetylation, as well as the biological relevance of Lys31 deacetylation and Lys5/Lys8 acetylation, needs further examination.

Besides acetylation, methylation is also an important PTM on histone H4. All methylations identified on BKPyV H4 were also found on host cell H4 except for the methylation on Arg3, which was detected only in BKPyV minichromosomes. As for formylation, all lysine residues found to be formylated were located in the histone H4 core domain, including Lys31, Lys59, Lys77, Lys79, and Lys91. We found that the lysine residues in histone H4's core domain could be either methylated or formylated; in contrast, the lysine residues in H4's N-terminal tail were mainly acetylated. When the overall acetylation level of histone H4 increased, the number of H4 lysine residues with either methylation or formylation decreased. Therefore, it is likely that H4 acetylation antagonize methylation and formylation. Since histone acetylation and methylation have been shown to regulate cellular activities, we expect histone lysine formylation to play an important role in cellular functions as well.

Table 2
Posttranslational modifications identified on histone H2B of BKPyV minichromosome and host Vero cells.

Subspecies	H2B-0[a]		H2B-1		H2B-2		H2B-3		H2B-4		H2B-5		H2B-6		H2B-7	
Modification Site	Vero	BKV	Vero	BKV	Vero	BKV	Vero	BKV	Vero	BKV	Vero	BKV	Vero	BKV	Vero	BKV
N-				Ac												
K5		Me[b]		Me		Ac	Me	Ac	Ac	Ac		Ac				
S6								Phos[f]								
K11										Ac			Ac			
K12								Ac	Ac	Ac	Ac	Ac	Ac	Ac	Ac	Ac
K15					Ac		Ac	Ac	Ac	Ac	Ac	Ac	Ac	Ac	Ac	Ac
K16				Ac	Ac		Ac	Ac	Ac	Ac	Ac	Ac	Ac	Ac	Ac	Ac
K20		Ac	Ac	Ac	Ac	Ac	Ac	Ac	Ac	Ac	Ac	Ac	Ac	Ac	Ac	Ac
K23							Ac	Ac	Ac	Ac	Ac	Ac	Ac	Ac	Ac	Ac
K34		Formyl		Formyl[e]		Ac, Formyl		Formyl		Formyl		Formyl				
K46								Ac								
R72	Me		Me			Me										
K108	Ubiq[c]		Ubiq					Ubiq, Me2[b]								
K116								Ac								
K120	Ac[d] Ubiq						Ac		Ac		Ac		Ac		Ac	

[a] Histone H4 subspecies (as labeled in Fig. 1C).
[b] Me: methylation; Me2: di-methylation.
[c] Ubiq: ubiquitination.
[d] Ac: acetylation.
[e] Formyl: formylation.
[f] Phos: phosphorylation.

Discussion

In the current study, we profiled the histone PTMs in BKPyV virions. Histone extracts from BKPyV virions and host Vero cells were first analyzed by TAU-PAGE, which separates proteins on the basis of molecular weight, charge, and affinity to Triton X-100 (Panyim and Chalkley, 1969), exploiting the fact that the charge states of histone variants and their subspecies are correlated with the PTMs they carry. The PTMs present on the TAU gel-resolved histone subspecies were further characterized by mass spectrometry analysis, a technique that is commonly used in the identification of PTMs because of the high sensitivity and accuracy of detection. By coupling TAU-PAGE separation with LC–MS/MS analysis, we were able to map the sites and forms of PTMs for all four core histones for both BKPyV virions and their host cells. Our results showed that the histone PTM profile of BKPyV virions is different from that of the host cells from which they originated. In addition, we found that the BKPyV minichromosome is hyperacetylated and carries more PTMs than host chromatin. We were able to identify sites of histone acetylation, methylation, ubiquitination, phosphorylation, and formylation in the BKPyV minichromosome, including several novel PTM sites.

In our present study, we observed one additional band for histone H2A in BKPyV virion extract as compared with Vero cell extract (western blot, Fig. 1B). Our analysis revealed more prominent histone acetylation in BKPyV minichromosomes than in host cells. The band shift observed in TAU-PAGE was demonstrated to be the N-acetylation of BKPyV histone H2A. The MS suggests that H2A-2 has K9 acetylation (Supplementary Fig. 3), but the antibody does not seem to be recognizing it (Supplementary Fig. 25). It may be due to the antibody with low specificity for K9 acetylation. In general, we think MS results are more convinced since they provide the accurate molecular weight as well as the peptide fragment ions information to confirm the presence of PTMs. The N-terminal acetylation of histone H2A has been suggested to function in the stabilization of nucleosome structure (Luger et al., 1997) and may further enhance protein stability in the BKPyV minichromosome. Additionally, we identified an ubiquitination at Lys119 of histone H2A in host cells but not in BKPyV virions. Lys119 is located in the C-terminus of histone H2A, close to the DNA exit and entry site (Luger et al., 1997). PTMs in the H2A C-terminus are known to affect nucleosome dynamics, stability, and binding with the linker histone H1 (Bonisch and Hake, 2012). Although a role has been proposed for H2A Lys119 ubiquitination in relieving suppressed RNA polymerase II elongation during transcription (Zhou et al., 2008), the PTM's biological relevance for BKPyV is currently unknown.

As for histone H2B, PTMs were found in the N-terminus, core domain, and C-terminus of BKPyV H2B based on our LC–MS/MS results. It has been suggested that PTMs in the N-terminal region of histones serve as a signal for the binding of non-histone proteins to chromatin, whereas PTMs in the histone core domain are involved in the structural changes of nucleosomes (Mersfelder and Parthun, 2006). We found two novel PTMs, Ser6 phosphorylation and Lys34 formylation, in the histone H2B of BKPyV minichromosomes but not in host H2B (Fig. 3); however, the biological significance of these modifications remains unclear. A study with yeast has suggested that repressor proteins can modulate lysine acetylation on histone H2B by means of binding to H2B residues 30 through 37 (Parra et al., 2006). Since we detected Lys34 formylation in histone H2B subspecies 0 through 5 but not in bands 6 and 7 (i.e., hyperacetylated forms of histone H2B) (Fig. 3), this formylation could be a signal code for regulatory protein binding that results in transcriptional activation.

The importance of both methylation and acetylation of histone H3 during viral infection has been reported in many studies, such as regulating the viral life cycle of EBV (Gerle et al., 2007) and the timing of HBV circular DNA replication (Bock et al., 2001). Histone H3 methylation and acetylation have also been found to be co-regulated; for example, an increased level of H3 Lys14 acetylation and H3 Lys4 methylation was accompanied by a decreased level of H3 Lys9 methylation in the HSV-1 promoter region (Kent et al., 2004). These known methylation and acetylation PTMs were also identified in our study. From a structural point of view, histone H3 Lys79 and histone H2B Lys120 are spatially close to each other in the histone octamer, and both of their side chains extend to the same surface of the nucleosome (Luger et al., 1997). H3 Lys79 methylation has been shown to be assisted by H2B Lys120 ubiquitination (Nguyen and Zhang, 2011). Our LC–MS/MS results indicated that both H2B Lys120 ubiquitination and H3 Lys79 methylation were present in BKV minichromosomes. This double PTM suggests that the minichromosomes of BKPyV virions are in a highly activated state.

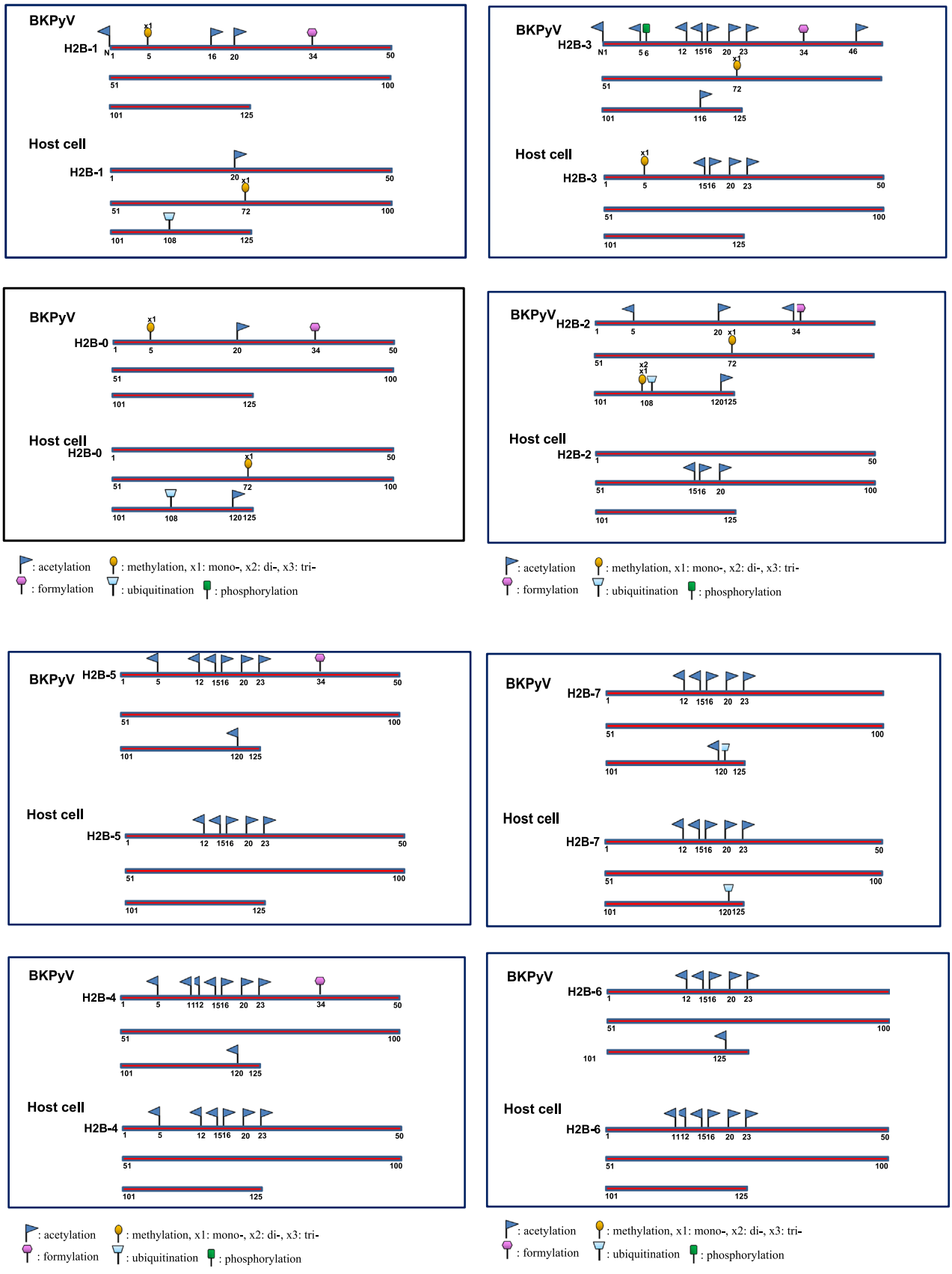

Fig. 3. Schematic illustration of histone modifications identified in histone H2B from BKPyV minichromosome and acid-extracted Vero cell histones.

Table 3
Posttranslational modifications identified on histone H3 of BKPyV minichromosome and host Vero cells.

Subspecies	H3-0[a]		H3-1		H3-2		H3-3		H3-4		H3-5		H3-6		H3-7	
Modification Site	Vero	BKV	Vero	BKV	Vero	BKV	Vero	BKV	Vero	BKV	Vero	BKV	Vero	BKV	Vero	BKV
K5						Me										
K9				Me Me2 Me3		Ac Me Me2 Me3		Ac Me Me2 Me3		Ac Me Me3		Ac Me Me2		Me Me2 Me3		Ac Me Me2 Me3
S10								Phos[d]						Phos		
K14				Ac		Ac	Ac	Ac		Ac	Ac	Ac		Ac		Ac
K18				Ac		Ac, Me		Ac		Ac		Ac		Ac		Ac
T22								Phos								
K23		Ac		Ac		Ac	Ac	Ac		Ac		Ac		Ac		Ac
K27	Ac[c] Me[b] Me2[b] Me3[b]	AcMe Me2	Ac Me Me2 Me3	Ac Me Me2	Ac Me, Me2 Me3	Me Me2	Me2 Me3	Ac Me Me2 Me3	Me Me2	Ac Me Me2 Me3	Ac Me Me2	Ac Me Me2 Me3	Ac Me Me2 Me3	Ac Me Me2 Me3	Ac Me Me2 Me3	Ac Me Me2 Me3
K36	Me Me2	Me Me2	Me2	Me Me2	Me	Me Me2	Me2	Ac Me Me2	Me		Me Me2	Me Me2	Me Me2	Ac Me Me2	Me Me2	
R42	Me		Me				Me						Me			
K56			Ac			Ac										
K79	Me Me2	Me	Me Me2	Me Me2	Me Me2	Me Me2		Me Me2	Me	Me	Me Me2	Me	Me Me2	Me Me2	Me Me2	Me

[a] Histone H3 subspecies (as labeled in Fig. 1D).
[b] Me: methylation; Me2: di-methylation; Me3: tri-methylation.
[c] Ac: acetylation.
[d] Phos: phosphorylation.

Histone phosphorylation is known to be involved in chromosome condensation (Gurley et al., 1978); for example, H3 Ser10 phosphorylation has been suggested to facilitate both chromosome condensation before cell division and chromatin decondensation for transcriptional activation (Cheung et al., 2000b; Nowak and Corces, 2004; Van Hooser et al., 1998). We detected H3 Ser10 phosphorylation in BKPyV virions. This phosphorylation has been suggested to regulate the viral assembly process (Dahl et al., 2007). We also found a novel site of histone H3 phosphorylation at Thr22. Since the threonine phosphorylation level of histone H3 was correlated with Gleason score of prostatic carcinomas (Metzger et al., 2008), the connection between this new threonine phosphorylation on the BKPyV minichromosome and prostate cancer should be further investigated.

Lysine acetylation is the most well studied PTM on histones. This modification alters the electrostatic properties of histones by neutralizing the positive charge on the ε-amino group of lysines (Grunstein, 1997). Acetylation plays a prominent role in the regulation of gene transcription (Allfrey et al., 1964; Allfrey and Mirsky, 1964). Many studies have focused on gene regulation associated with specific acetylation sites on histone H4. For example, histone H4 Lys16 acetylation was shown to affect chromatin compaction and gene transcription (Shogren-Knaak and Peterson, 2006). In the structure of the histone octamer, the Lys16 side chain of the histone H4 subunit extends to the surface of histone H2A and H2B subunits; thus, modification of H4 Lys16 by acetylation has structurally relevant consequences (Luger et al., 1997). Acetylation could occur on multiple lysine residues of histone H4, and we found Lys12, Lys8, and Lys5 to be acetylated in both BKPyV H4 and host cell H4. The combinatorial PTMs on these four sites are read by effector proteins that convert chromatin to a highly active state (Mujtaba et al., 2007). As for the acetylation at histone H4 Lys31, it was only found in hypoacetylated forms of BKPyV histone H4, suggesting that H4 Lys31 acetylation had to take place before H4 Lys16 acetylation. On the basis of this finding, we hypothesize that the deacetylation of H4 Lys31 is required for the conversion of chromatin to a highly active state, as well as for the subsequent H4 acetylations at Lys16, Lys12, Lys8, and Lys5.

A similar acetylation mechanism was also observed among five lysine residues in BKPyV histone H3. Acetylation initially occurred on Lys23/Lys27, followed by Lys14/Lys18, and finally on Lys9 (Fig. 4). Histone H3 Lys14 acetylation is known to be tightly involved in cell cycle regulation, cell proliferation, and apoptosis and is indispensable for the dissociation of histone octamers from promoter DNA (Luebben et al., 2010). H3 Lys14 and Lys27 acetylations are associated with active enhancers (Creyghton et al., 2010; Rada-Iglesias et al., 2011; Zentner et al., 2011), and H3 Lys18 and Lys27 acetylations have been suggested to be histone activation marks (Jin et al., 2011). Based on our results, we suggest that H3 Lys27 acetylation could be a gene activation switch that recruits histone acetylation transferases to acetylate other lysine residues. However, methylation could also take place on H3 Lys27, and this methylation has been associated with latency for EBV, Kaposi sarcoma-associated herpesvirus, and HIV (Gunther and Grundhoff, 2010; Kim et al., 2011; Murata et al., 2012). Since H3 Lys27 acetylation and methylation are antagonistic in regulating the active state of chromatin, we cannot conclude as to whether virion-derived BKPyV minichromosomes were in an active state, because both acetylation and methylation were identified at H3 Lys27 in our LC – MS/MS results (Fig. 4).

In addition to acetylation and methylation, formylation is another possible histone PTM on lysine residues and has recently been reported to occur in the histone tail and globular domain regions (Garcia et al., 2006; Wisniewski et al., 2007). Formylation and acetylation/methylation are antagonistic, as they usually take place at the same lysine residue on histones. Therefore, formylation is suggested to participate in the regulation of chromatin functions. Our results showed that the level of histone H4 formylation was higher in host cells than in BKPyV minichromosomes. In other words, compared with host chromatin, the BKPyV minichromosome was in a more active state due to the presence of more highly acetylated/methylated forms of H4. This observation is consistent with the previous finding that the SV40 minichromosome has higher replication and transcription efficiency than host chromatin (Alexiadis et al., 1997). Therefore, we hypothesize that the antagonistic relationship between formylation and acetylation/methylation may be a key factor in chromatin regulation.

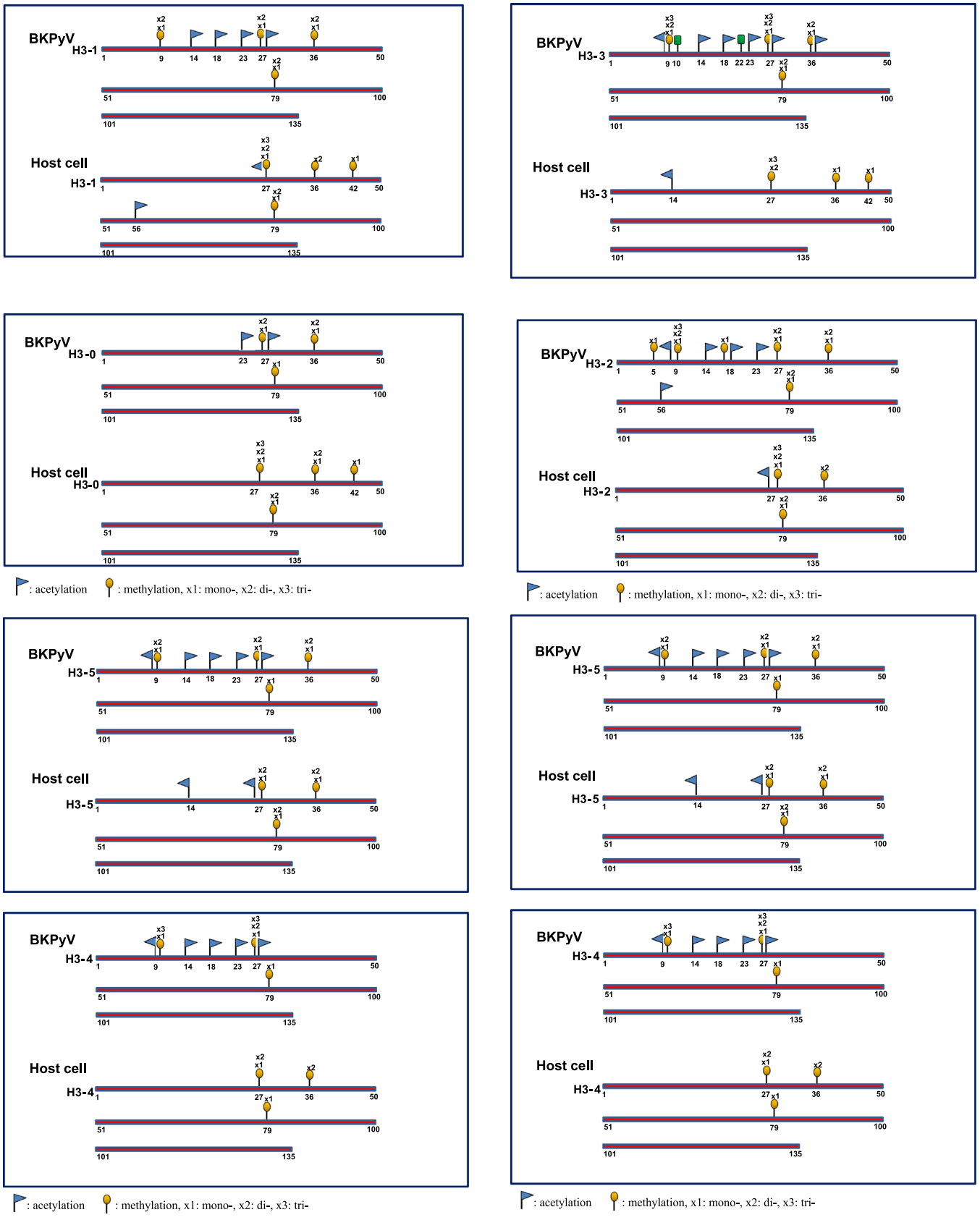

Fig. 4. Schematic illustration of histone modifications identified in histone H3 from BKPyV minichromosome and acid-extracted Vero cell histones.

Arginine residues can also be modified by methylation. In the current study, a mono-methylation was identified on Arg3 of histone H4 from BKPyV virions. However, only di-methylation has been reported previously for H4 Arg3, and this arginine di-methylation can be either the symmetric or the asymmetric type. It has been shown that symmetric di-methylation of histone H4

Table 4
Posttranslational modifications identified on histone H4 of BKPyV minichromosome and host Vero cells.

Subspecies	H4-0[a]		H4-1		H4-2		H4-3		H4-4	
Modification Site	Vero	BKV	Vero	BKV	Vero	BKV	Vero	BKV	Vero	BKV
N-					Ac			Ac		
R3								Me		
K5							Ac	Ac	Ac	Ac
K8				Ac	Ac	Ac	Ac	Ac	Ac	Ac
K12	Ac[c]	Ac	Ac	Ac	Ac	Ac	Ac	Ac	Ac	Ac
K16	Ac	Ac	Ac	Ac	Ac	Ac	Ac	Ac	Ac	Ac
K20		Me2	Me	Me2	Me2	Me2	Me2			
R23	Me[b], Me2[b]	Me2		Me2	Me2	Me2				
K31	Ac, Formyl[d]	Ac, Formyl	Formyl	Ac, Formyl	Formyl	Formyl		Formyl		
R55	Me	Me	Me	Me	Me	Me		Me		
K59		Formyl	Ac, Formyl	Formyl		Formyl				
K77	Me	Me, Formyl	Formyl	Me, Formyl	Formyl	Me				
K79	Formyl		Formyl							
K91	Formyl									

[a] Histone H4 subspecies (as labeled in Fig. 1E).
[b] Me: methylation; Me2: di-methylation.
[c] Ac: acetylation.
[d] Formyl: formylation.

Arg3 could repress gene expression (Zhao et al., 2009), whereas asymmetric di-methylation at the same position serves as a gene activation signal (Li et al., 2010). Another study demonstrated that the Arg3-di-methylated histone H4 found in EBV-transformed lymphoblastoid cell lines may bind to unmethylated promoters and suppress gene expression (Majumder et al., 2010). Moreover, the di-methylation on histone H4 Arg3 was found to be at first symmetrical and later transformed into the asymmetric type in the developing mouse cortex (Chittka, 2010). The Arg3 methylation of histone 4 has also been shown to facilitate the subsequent acetylation of H4 at Lys9 and Lys14 (Li et al., 2010). Since mono-methylation is an intermediate of arginine di-methylation, the newly identified Arg3 mono-methylation on BKPyV H4 might also play an important role in regulating the life cycle of BKPyV.

Hyperacetylated histones H3 and H4 have been suggested to be randomly distributed in the polyomaviral genome (Carbone et al., 2004), but the modification type and the amino acid residues modified remain unclear. Here, we have achieved a comprehensive identification of all histone PTMs in BKPyV minichromosomes and in host Vero cells by the LC−MS/MS method. We have shown histones from BKPyV minichromosomes to be hyperacetylated and to contain more methylations than those from host cells, suggesting a more active state of the BKPyV minichromosome relative to host chromatin. However, more information is required to elucidate the responsible mechanisms at work during BKPyV infection. The distribution of histones changes dynamically in the regulatory region of the viral genome during the early and late phases of SV40 infection (Carbone et al., 2004). Proteomics tools have the power not only to examine the varying histone distributions in different viral intermediates in BKPyV infected cells but also to further investigate the correlations between histone redistributions and histone PTMs. Moreover, histone H1 is present in viral intermediate minichromosomes in polyomavirus-infected cells but not in mature virions, and the removal of H1 has been shown to occur during the viral assembly process. Thus, further research on histone PTM changes could contribute to a more detailed understanding of the viral assembly process. Finally, we report the different observed BKPyV and host histone PTMs from the present study in a qualitatively manner, as we did not perform quantitative analysis for each PTM detected. In future studies, quantitative proteomics tools may be applied to provide more detailed information on epigenetic regulation in viral life cycles.

Materials and methods

BKPyV propagation

Cell culture and BKPyV propagation were performed as described in our previous report (Fang et al., 2010). Briefly, Vero cells were infected with BKPyV (UT strain, a generous gift from Dr. W. Atwood, Brown University). When the cytopathic effect became evident after 4 weeks of infection, the medium containing cell lysate was collected by centrifugation and the cell pellet was used as the source of BKPyV particles for purification.

BKPyV purification

The BKPyV purification procedures were similar to that described in our previous report (Fang et al., 2010). Briefly, the BKPyV-infected cell pellet described above was resuspended in Tris-buffered saline and incubated with type V neuraminidase. The cell debris was removed by centrifugation and the virus-containing supernatant was concentrated by a 20% sucrose cushion. The virus was further purified by the CsCl gradient centrifugation.

Extraction of Histones

BKPyV-infected Vero cells were pelleted by centrifugation at 200*g* for 10 min at 4 °C, washed twice with iced-cold phosphate-buffered saline, and then resuspended in 10 cell volumes of hypotonic lysis buffer (0.5% [v/v] Triton X-100, 2 mM phenylmethylsulfonyl fluoride), followed by centrifugation at 200*g* for 10 min at 4 °C. After the removal of the supernatant, the pellet, named crude chromatin extract, was incubated in 0.2 N HCl for 3 h at 4 °C, followed by centrifugation at 11,000*g* for 10 min at 4 °C. The supernatant was kept for further histone analysis.

Triton-acetic acid-urea (TAU) polyacrylamide gel electrophoresis (PAGE)

TAU-PAGE (Schaffhausen and Benjamin, 1976) was applied to separate different isoforms of histones H2A, H2B, H3, and H4. TAU gels were prepared with a stacking gel containing 4% acrylamide/bis-acrylamide, 8 M urea, and 5% acetic acid, and a separating gel containing 15% acrylamide/bis-acrylamide, 8 M urea, 0.4% Triton

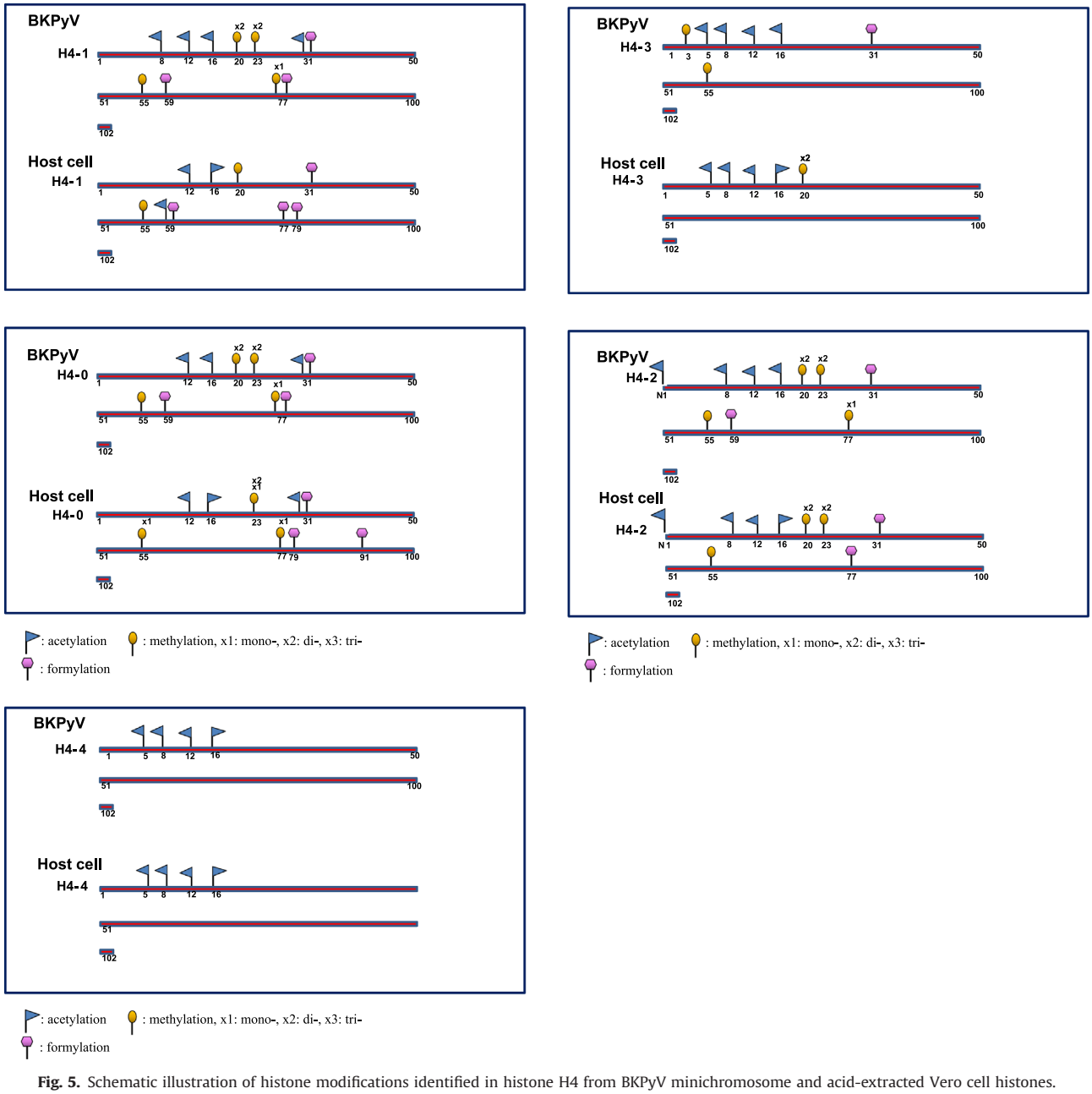

Fig. 5. Schematic illustration of histone modifications identified in histone H4 from BKPyV minichromosome and acid-extracted Vero cell histones.

X-100, and 5% acetic acid. Acid-extracted histones were dissolved in sample buffer (6 M urea, 5% acetic acid, 2% β-mercaptoethanol, 10 mg/mL protamine) and subjected to TAU gel electrophoresis at 300 V at 4 °C until the marker, cytochrome c (Sigma, St. Louis, MO), had migrated through 80% of the gel length (approximately 36 h), at which point electrophoresis was stopped for further analysis of the resolved histone bands.

Western blotting

Initially, the acid extracted cellular histones and the purified virus was resolved by 15% TAU-PAGE. The proteins were then transferred to a polyvinylidene fluoride (PVDF) membrane (Pall, East Hills, NY, USA) using a semi-dry electroblotting system (Thermo Fisher Scientific,Waltham, MA, USA) at 1 mA/cm^2 for 60 min. Histones were detected using anti-histone H2A, H2B, H3, H4 (Upstate, Lake Placid, NY, USA) and H2A lysine 9 acetylation (Abcam Cambridge, UK) antibodies. Bands were detected using an anti-IgG polyclonal antibody conjugated to peroxidase (Santa Cruz Biotechnology), followed by exposure to a chemiluminescent substrate (PerkinElmer Life Sciences, Foster City, CA, USA). The results were detected using BioSpectrum Imaging System (UVP, Bio-Rad Laboratories, Hercules, CA, USA).

Sample preparation for mass spectrometry (MS) analysis

Protein samples were subjected to enzyme digestion according to the following procedure. After thermal denaturation at 95 °C for 5 min, protein samples (0.1 mg/ml) were reduced through the addition of dithiothreitol (DTT) (10 mM final). Alkylation was performed by adding iodoacetic acid (20 mM final) and incubating the samples for 30 min at room temperature in the dark, followed by the addition of a second aliquot of DTT to quench the reaction. Trypsin solution (20 ng/μl) was then added to the protein samples at a 1:50 (w/w) ratio, and the reactions were incubated at 25 °C for 30 min. The enzymatic digestions were quenched by the addition

of 10 μl of 10% formic acid, and digested peptides were dried in a speed-vac prior to mass analysis.

Liquid chromatography–mass spectrometry (nanoflow LC–MS/MS)

High-resolution, high-mass accuracy nanoflow LC–MS/MS was performed on a combined linear quadrupole ion trap (LTQ) and Fourier transform ion cyclotron resonance (FT-ICR) mass spectrometer (LTQ-FT system, Thermo Fisher Scientific, Waltham, MA) equipped with a nanoelectrospray ion source (New Objective, Woburn, MA), an Agilent 1100 Series binary high-performance liquid chromatography pump (Agilent Technologies, Palo Alto, CA), and a Famos autosampler (LC Packings, San Francisco, CA). Each digested peptide solution was injected onto a self-packed pre-column (150 μm ID × 20 mm, 5 μm, 200 Å). Chromatographic separation was performed on a self-packed reverse-phase C18 nanocolumn (75 μm ID × 150 mm, 5 μm, 100 Å) using 0.1% formic acid in water (mobile phase A) and 0.1% formic acid in 80% acetonitrile (mobile phase B). This was done by applying a linear gradient from 5% to 40% mobile phase B for 40 min at a flow rate of 300 nl/min provided across a flow splitter by the HPLC pumps. Electrospray voltage was applied at 2 kV, and capillary temperature was set at 200 °C. A scan cycle was initiated with a full-scan survey MS spectrum (*m/z* 300–2000); this was performed on the FT-ICR mass spectrometer with a resolution of 100,000 (at *m/z* 400). The 10 most abundant ions detected in the scan were subjected to MS/MS analysis performed in the LTQ mass spectrometer. Ion accumulation (Auto Gain Control target number) and maximal ion accumulation time for full-scan and MS/MS modes were set at 1×10^6 ions, 1,000 ms and 5×10^4 ions, 200 ms, respectively. The parameters for collision-induced dissociation were set at 35% normalized collision energy, 0.3 activation Q, and 30 ms activation time.

For data analysis, all MS/MS spectra were converted from RAW to mzXML and MGF formats by using MM File Conversion Tools ((Xu and Freitas, 2009) http://www.massmatrix.net) and then analyzed by MassMatrix (Xu et al., 2010) for MS/MS ion search. The search parameters in MassMatrix included error tolerances of 10 ppm and 0.6 Da for precursor ions and MS/MS fragment ions, respectively; trypsin as the enzyme; and a missed cleavage number of 3. The variable PTMs in the search parameters were assigned to include the oxidation of methionine, carbamidomethylation of cysteine, phosphorylation of serine/threonine/tyrosine, methylation of lysine/arginine, and acetylation of lysine.

Acknowledgments

* We thank Drs. Ming-Daw Tsai (Institute of Biological Chemistry, Academia Sinica) and Li-Jung Juan (Genomics Research Center, Academia Sinica) for insightful suggestions and discussions. Mass spectra data were collected at the Mass Spectrometry Facility of Genomics Research Center, Academia Sinica. This work was supported by research grants from the National Science Council, NSC 100–2113-M-019-002-MY2, NSC 101–2320-B-194-002-MY3, NSC 102–2311-B-705-001 and Chia-Yi Christian Hospital, R101-11, Taiwan, ROC.

Appendix. Supporting information

Supplementary data associated with this article can be found in the online version at http://dx.doi.org/10.1016/j.virol.2015.04.009.

References

Alexiadis, V., Halmer, L., Gruss, C., 1997. Influence of core histone acetylation on SV40 minichromosome replication in vitro. Chromosoma 105, 324–331.
Allfrey, V.G., Faulkner, R., Mirsky, A.E., 1964. Acetylation and methylation of histones and their possible role in the regulation of RNA synthesis. Proc. Natl. Acad. Sci. USA 51, 786–794.
Allfrey, V.G., Mirsky, A.E., 1964. Structural modifications of histones and their possible role in the regulation of RNA synthesis. Science 144, 559.
Balakrishnan, L., Gefroh, A., Milavetz, B., 2010. Histone H4 lysine 20 mono- and trimethylation define distinct biological processes in SV40 minichromosomes. Cell Cycle 9, 1320–1332.
Balakrishnan, L., Milavetz, B., 2005. Programmed remodeling of hyperacetylated histone H4 and H3 organization on the SV40 genome during lytic infection. Virology 334, 111–123.
Belloni, L., Pollicino, T., De Nicola, F., Guerrieri, F., Raffa, G., Fanciulli, M., Raimondo, G., Levrero, M., 2009. Nuclear HBx binds the HBV minichromosome and modifies the epigenetic regulation of cccDNA function. Proc. Natl. Acad. Sci. USA 106, 19975–19979.
Bock, C.T., Schranz, P., Schroder, C.H., Zentgraf, H., 1994. Hepatitis B virus genome is organized into nucleosomes in the nucleus of the infected cell. Virus Genes 8, 215–229.
Bock, C.T., Schwinn, S., Locarnini, S., Fyfe, J., Manns, M.P., Trautwein, C., Zentgraf, H., 2001. Structural organization of the hepatitis B virus minichromosome. J. Mol. Biol. 307, 183–196.
Bonisch, C., Hake, S.B., 2012. Histone H2A variants in nucleosomes and chromatin: more or less stable? Nucleic Acids Res. 40, 10719–10741.
Britton, L.M., Gonzales-Cope, M., Zee, B.M., Garcia, B.A., 2011. Breaking the histone code with quantitative mass spectrometry. Expert Rev. Proteomics 8, 631–643.
Broekema, N.M., Imperiale, M.J., 2013. miRNA regulation of BK polyomavirus replication during early infection. Proc. Natl. Acad. Sci. USA 110, 8200–8205.
Carbone, M., Ascione, G., Chichiarelli, S., Garcia, M.I., Eufemi, M., Amati, P., 2004. Chromosome-protein interactions in polyomavirus virions. J. Virol. 78, 513–519.
Chang, C.F., Wang, M., Fang, C.Y., Chen, P.L., Wu, S.F., Chan, M.W., Chang, D., 2011. Analysis of DNA methylation in human BK virus. Virus Genes 43, 201–207.
Chestier, A., Yaniv, M., 1979. Rapid turnover of acetyl groups in the four core histones of simian virus 40 minichromosomes. Proc. Natl. Acad. Sci. USA 76, 46–50.
Cheung, P., Allis, C.D., Sassone-Corsi, P., 2000a. Signaling to chromatin through histone modifications. Cell 103, 263–271.
Cheung, P., Tanner, K.G., Cheung, W.L., Sassone-Corsi, P., Denu, J.M., Allis, C.D., 2000b. Synergistic coupling of histone H3 phosphorylation and acetylation in response to epidermal growth factor stimulation. Mol. Cell 5, 905–915.
Chittka, A., 2010. Dynamic distribution of histone H4 arginine 3 methylation marks in the developing murine cortex. PLoS One 5, e13807.
Creyghton, M.P., Cheng, A.W., Welstead, G.G., Kooistra, T., Carey, B.W., Steine, E.J., Hanna, J., Lodato, M.A., Frampton, G.M., Sharp, P.A., Boyer, L.A., Young, R.A., Jaenisch, R., 2010. Histone H3K27ac separates active from poised enhancers and predicts developmental state. Proc. Natl. Acad. Sci. USA 107, 21931–21936.
Dahl, J., Chen, H.I., George, M., Benjamin, T.L., 2007. Polyomavirus small T antigen controls viral chromatin modifications through effects on kinetics of virus growth and cell cycle progression. J. Virol. 81, 10064–10071.
Deshmane, S.L., Fraser, N.W., 1989. During latency, herpes simplex virus type 1 DNA is associated with nucleosomes in a chromatin structure. J. Virol. 63, 943–947.
Fang, C.Y., Chen, H.Y., Wang, M., Chen, P.L., Chang, C.F., Chen, L.S., Shen, C.H., Ou, W. C., Tsai, M.D., Hsu, P.H., Chang, D., 2010. Global analysis of modifications of the human BK virus structural proteins by LC–MS/MS. Virology 402, 164–176.
Favre, M., Breitburd, F., Croissant, O., Orth, G., 1977. Chromatin-like structures obtained after alkaline disruption of bovine and human papillomaviruses. J. Virol. 21, 1205–1209.
Garcia, B.A., Joshi, S., Thomas, C.E., Chitta, R.K., Diaz, R.L., Busby, S.A., Andrews, P.C., Ogorzalek Loo, R.R., Shabanowitz, J., Kelleher, N.L., Mizzen, C.A., Allis, C.D., Hunt, D.F., 2006. Comprehensive phosphoprotein analysis of linker histone H1 from *Tetrahymena thermophila*. Mol. Cell Proteomics 5, 1593–1609.
Gerle, B., Koroknai, A., Fejer, G., Bakos, A., Banati, F., Szenthe, K., Wolf, H., Niller, H. H., Minarovits, J., Salamon, D., 2007. Acetylated histone H3 and H4 mark the upregulated LMP2A promoter of Epstein–Barr virus in lymphoid cells. J. Virol. 81, 13242–13247.
Gilmore, J.M., Washburn, M.P., 2007. Deciphering the combinatorial histone code. Nat. Methods 4, 480–481.
Griffith, J.D., 1975. Chromatin structure: deduced from a minichromosome. Science 187, 1202–1203.
Grunstein, M., 1997. Histone acetylation in chromatin structure and transcription. Nature 389, 349–352.
Gunther, T., Grundhoff, A., 2010. The epigenetic landscape of latent Kaposi sarcoma-associated herpesvirus genomes. PLoS Pathog. 6, e1000935.
Gurley, L.R., D'Anna, J.A., Barham, S.S., Deaven, L.L., Tobey, R.A., 1978. Histone phosphorylation and chromatin structure during mitosis in Chinese hamster cells. Eur. J. Biochem. 84, 1–15.
Jenuwein, T., Allis, C.D., 2001. Translating the histone code. Science 293, 1074–1080.
Jin, Q., Yu, L.R., Wang, L., Zhang, Z., Kasper, L.H., Lee, J.E., Wang, C., Brindle, P.K., Dent, S.Y., Ge, K., 2011. Distinct roles of GCN5/PCAF-mediated H3K9ac and CBP/p300-mediated H3K18/27ac in nuclear receptor transactivation. EMBO J. 30, 249–262.

Kent, J.R., Zeng, P.Y., Atanasiu, D., Gardner, J., Fraser, N.W., Berger, S.L., 2004. During lytic infection herpes simplex virus type 1 is associated with histones bearing modifications that correlate with active transcription. J. Virol. 78, 10178–10186.
Kim, H.G., Kim, K.C., Roh, T.Y., Park, J., Jung, K.M., Lee, J.S., Choi, S.Y., Kim, S.S., Choi, B. S., 2011. Gene silencing in HIV-1 latency by polycomb repressive group. Virol. J. 8, 179.
Kornberg, R.D., 1974. Chromatin structure: a repeating unit of histones and DNA. Science 184, 868–871.
Kornberg, R.D., Lorch, Y., 1999. Twenty-five years of the nucleosome, fundamental particle of the eukaryote chromosome. Cell 98, 285–294.
Kouzarides, T., 2007. Chromatin modifications and their function. Cell 128, 693–705.
Leinbach, S.S., Summers, W.C., 1980. The structure of herpes simplex virus type 1 DNA as probed by micrococcal nuclease digestion. J. Gen. Virol. 51, 45–59.
Li, X., Hu, X., Patel, B., Zhou, Z., Liang, S., Ybarra, R., Qiu, Y., Felsenfeld, G., Bungert, J., Huang, S., 2010. H4R3 methylation facilitates beta-globin transcription by regulating histone acetyltransferase binding and H3 acetylation. Blood 115, 2028–2037.
Luebben, W.R., Sharma, N., Nyborg, J.K., 2010. Nucleosome eviction and activated transcription require p300 acetylation of histone H3 lysine 14. Proc. Natl. Acad. Sci. USA 107, 19254–19259.
Luger, K., Mader, A.W., Richmond, R.K., Sargent, D.F., Richmond, T.J., 1997. Crystal structure of the nucleosome core particle at 2.8 A resolution. Nature 389, 251–260.
Majumder, S., Alinari, L., Roy, S., Miller, T., Datta, J., Sif, S., Baiocchi, R., Jacob, S.T., 2010. Methylation of histone H3 and H4 by PRMT5 regulates ribosomal RNA gene transcription. J. Cell. Biochem. 109, 553–563.
Mersfelder, E.L., Parthun, M.R., 2006. The tale beyond the tail: histone core domain modifications and the regulation of chromatin structure. Nucleic Acids Res. 34, 2653–2662.
Metzger, E., Yin, N., Wissmann, M., Kunowska, N., Fischer, K., Friedrichs, N., Patnaik, D., Higgins, J.M., Potier, N., Scheidtmann, K.H., Buettner, R., Schule, R., 2008. Phosphorylation of histone H3 at threonine 11 establishes a novel chromatin mark for transcriptional regulation. Nat. Cell Biol. 10, 53–60.
Milavetz, B., 2004. Hyperacetylation and differential deacetylation of histones H4 and H3 define two distinct classes of acetylated SV40 chromosomes early in infection. Virology 319, 324–336.
Milavetz, B., Kallestad, L., Gefroh, A., Adams, N., Woods, E., Balakrishnan, L., 2012. Virion-mediated transfer of SV40 epigenetic information. Epigenetics 7, 528–534.
Muggeridge, M.I., Fraser, N.W., 1986. Chromosomal organization of the herpes simplex virus genome during acute infection of the mouse central nervous system. J. Virol. 59, 764–767.
Mujtaba, S., Zeng, L., Zhou, M.M., 2007. Structure and acetyl-lysine recognition of the bromodomain. Oncogene 26, 5521–5527.
Murata, T., Kondo, Y., Sugimoto, A., Kawashima, D., Saito, S., Isomura, H., Kanda, T., Tsurumi, T., 2012. Epigenetic histone modification of Epstein – Barr virus BZLF1 promoter during latency and reactivation in Raji cells. J. Virol. 86, 4752–4761.
Nguyen, A.T., Zhang, Y., 2011. The diverse functions of Dot1 and H3K79 methylation. Genes Dev. 25, 1345–1358.
Nowak, S.J., Corces, V.G., 2004. Phosphorylation of histone H3: a balancing act between chromosome condensation and transcriptional activation. Trends Genet. 20, 214–220.
Panyim, S., Chalkley, R., 1969. High resolution acrylamide gel electrophoresis of histones. Arch. Biochem. Biophys. 130, 337–346.
Parra, M.A., Kerr, D., Fahy, D., Pouchnik, D.J., Wyrick, J.J., 2006. Deciphering the roles of the histone H2B N-terminal domain in genome-wide transcription. Mol. Cell Biol. 26, 3842–3852.
Pollicino, T., Belloni, L., Raffa, G., Pediconi, N., Squadrito, G., Raimondo, G., Levrero, M., 2006. Hepatitis B virus replication is regulated by the acetylation status of hepatitis B virus cccDNA-bound H3 and H4 histones. Gastroenterology 130, 823–837.
Prieto-Soto, A., Gourlie, B., Miwa, M., Pigiet, V., Sugimura, T., Malik, N., Smulson, M., 1983. Polyoma virus minichromosomes: poly ADP-ribosylation of associated chromatin proteins. J. Virol. 45, 600–606.
Rada-Iglesias, A., Bajpai, R., Swigut, T., Brugmann, S.A., Flynn, R.A., Wysocka, J., 2011. A unique chromatin signature uncovers early developmental enhancers in humans. Nature 470, 279–283.
Ramos, E., Drachenberg, C.B., Portocarrero, M., Wali, R., Klassen, D.K., Fink, J.C., Farney, A., Hirsch, H., Papadimitriou, J.C., Cangro, C.B., Weir, M.R., Bartlett, S.T., 2002. BK virus nephropathy diagnosis and treatment: experience at the University of Maryland Renal Transplant Program. Clin. Transpl., 143–153.
Ramos, E., Hirsch, H.H., 2006. Polyomavirus-associated nephropathy: updates on a persisting challenge. Transpl. Infect. Dis. 8, 59–61.
Rosl, F., Waldeck, W., Zentgraf, H., Sauer, G., 1986. Properties of intracellular bovine papillomavirus chromatin. J. Virol. 58, 500–507.
Schaffhausen, B.S., Benjamin, T.L., 1976. Deficiency in histone acetylation in nontransforming host range mutants of polyoma virus. Proc. Natl. Acad. Sci. USA 73, 1092–1096.
Shaw, J.E., Levinger, L.F., Carter Jr., C.W., 1979. Nucleosomal structure of Epstein – Barr virus DNA in transformed cell lines. J. Virol. 29, 657–665.
Shogren-Knaak, M., Peterson, C.L., 2006. Switching on chromatin: mechanistic role of histone H4-K16 acetylation. Cell Cycle 5, 1361–1365.
Strahl, B.D., Allis, C.D., 2000. The language of covalent histone modifications. Nature 403, 41–45.
Tan, K.B., 1977. Histones: metabolism in simian virus 40-infected cells and incorporation into virions. Proc. Natl. Acad. Sci. USA 74, 2805–2809.
Tate, V.E., Philipson, L., 1979. Parental adenovirus DNA accumulates in nucleosome-like structures in infected cells. Nucleic Acids Res. 6, 2769–2785.
Van Hooser, A., Goodrich, D.W., Allis, C.D., Brinkley, B.R., Mancini, M.A., 1998. Histone H3 phosphorylation is required for the initiation, but not maintenance, of mammalian chromosome condensation. J. Cell. Sci. 111, 3497–3506, Pt 23.
Waga, S., Stillman, B., 1998. The DNA replication fork in eukaryotic cells. Annu. Rev. Biochem. 67, 721–751.
Wang, Z., Patel, D.J., 2011. Combinatorial readout of dual histone modifications by paired chromatin-associated modules. J. Biol. Chem. 286, 18363–18368.
Wisniewski, J.R., Zougman, A., Kruger, S., Mann, M., 2007. Mass spectrometric mapping of linker histone H1 variants reveals multiple acetylations, methylations, and phosphorylation as well as differences between cell culture and tissue. Mol. Cell. Proteomics 6, 72–87.
Wooldridge, T.R., Laimins, L.A., 2008. Regulation of human papillomavirus type 31 gene expression during the differentiation-dependent life cycle through histone modifications and transcription factor binding. Virology 374, 371–380.
Xu, H., Freitas, M.A., 2009. MassMatrix: a database search program for rapid characterization of proteins and peptides from tandem mass spectrometry data. Proteomics 9, 1548–1555.
Xu, H., Hsu, P.H., Zhang, L., Tsai, M.D., Freitas, M.A., 2010. Database search algorithm for identification of intact cross-links in proteins and peptides using tandem mass spectrometry. J. Proteome Res. 9, 3384–3393.
Zentner, G.E., Tesar, P.J., Scacheri, P.C., 2011. Epigenetic signatures distinguish multiple classes of enhancers with distinct cellular functions. Genome Res. 21, 1273–1283.
Zhang, L., Su, X., Liu, S., Knapp, A.R., Parthun, M.R., Marcucci, G., Freitas, M.A., 2007. Histone H4 N-terminal acetylation in Kasumi-1 cells treated with depsipeptide determined by acetic acid-urea polyacrylamide gel electrophoresis, amino acid coded mass tagging, and mass spectrometry. J. Proteome Res. 6, 81–88.
Zhao, Q., Rank, G., Tan, Y.T., Li, H., Moritz, R.L., Simpson, R.J., Cerruti, L., Curtis, D.J., Patel, D.J., Allis, C.D., Cunningham, J.M., Jane, S.M., 2009. PRMT5-mediated methylation of histone H4R3 recruits DNMT3A, coupling histone and DNA methylation in gene silencing. Nat. Struct. Mol. Biol. 16, 304–311.
Zhou, W., Zhu, P., Wang, J., Pascual, G., Ohgi, K.A., Lozach, J., Glass, C.K., Rosenfeld, M. G., 2008. Histone H2A monoubiquitination represses transcription by inhibiting RNA polymerase II transcriptional elongation. Mol. Cell 29, 69–80.